Evaporative Resistance is of Equal Importance as Surface Albedo in High Latitude Surface Temperatures Due to Cloud Feedbacks

Jinhyuk E. Kim[1], Marysa M. Laguë[1,2], Sam Pennypacker[1], Eliza Dawson[1,3], Abigail L.S. Swann[1,4]

[1]Department of Atmospheric Sciences, University of Washington, Seattle, WA 98195, USA
[2]Now at Department of Earth and Planetary Science, University of California Berkeley, Berkeley, CA 94709, USA
[3]Now at School of Earth, Energy, and Environmental Sciences, Stanford University, Stanford, CA 94305, USA
[4]Department of Biology, University of Washington, Seattle, WA 98195, USA

Key Points:

- Two Arctic plant types with different properties cause substantial changes to land surface temperature through different physical pathways
- Reducing land surface evaporative resistance increases low clouds and increases shortwave cloud forcing
- Albedo directly warms the land surface, while changes in evaporation warms mostly by modifying cloud cover

Corresponding author: Abigail Swann, `aswann@uw.edu`

Corresponding author: Jinhyuk Kim, `jinhyukekim@gmail.com`

Abstract

Arctic vegetation is known to influence Arctic surface temperatures through albedo. However, it is less clear how plant evaporative resistance and albedo independently influence surface climate at high latitudes. We use surface properties derived from two common Arctic tree types to simulate the climate response to a change in land surface albedo and evaporative resistance in factorial combinations. We find that lower evaporative resistances lead to an increase of low clouds. The reflection of light due to the difference in albedos between vegetation types is similar to the loss of incident sunlight due to increased cloud cover resulting from lower evaporative resistance from vegetation change. Our results demonstrate that realistic changes in evaporative resistance can have an equal impact on surface temperature to changes in albedo, and that cloud feedbacks play a first order role in determining the surface climate response to changes in Arctic land cover.

Plain Language Summary

In the Arctic, darker land surfaces lead to warmer temperatures because they absorb more sunlight. However, there are multiple types of plants that grow in the Arctic, which differ not only in how dark they are but also how easily they release water. We investigate how different Arctic plants' absorption of sunlight and ability to release water to the atmosphere can affect temperature over Arctic land using an Earth System Model. We find that dark trees are capable of absorbing a greater fraction of the incoming sunlight than their brighter counterparts, which tends to warm the surface. In comparison, when the land surface has a harder time releasing water into the atmosphere, a smaller fraction of energy at the land surface is used to evaporate water. This warms the air above the surface, which leads to evaporation of cloud droplets and less cloud cover. As a result, more sunlight is able to reach the surface, and land surface temperatures are warmer even when the surface is relatively bright. In combination, we find that the darkness of the surface and the plants' ability to release water have an equal influence on surface temperatures over land in the Arctic.

1 Introduction

As the concentrations of atmospheric CO_2 and other greenhouse gases rise, global temperatures will continue to increase, with even larger increases at high latitudes (Collins et al., 2013). We expect that higher Arctic temperatures will lead to a poleward expansion of the tree-line (Gallimore et al., 2005; Lloyd, 2005; Jeong et al., 2011; Falloon et al., 2012). Tree-line expansion has already been observed in Alaska (Rupp et al., 2000; Lloyd, 2005) and in Sweden(Rundqvist et al., 2011). With continued warming, simulations of future climate scenarios suggest an increase in shrubs and needleleaf trees in the Arctic (Jeong et al., 2011; Falloon et al., 2012).

In addition to the current and future poleward expansion of trees at high northern latitudes, there is evidence from paleo records of expanded forest cover during past warm periods. Climate model simulations set with Mid-Holocene conditions show an expansion of boreal forest into the tundra relative to preindustrial-like conditions (Gallimore et al., 2005). There is also observational evidence for forests in the Arctic in the Late Cretaceous up to the Paleocene with deciduous trees occupying the land above 65°N (Wolfe & Upchurch, 1987; Royer et al., 2006). Along with the increased northward extent of these prehistoric forests, there are indications that these forests were deciduous, rather than the high-latitude needleleaf forests of the present day (G. Bonan, 2015).

Boreal forest communities are comprised of both needleleaf evergreen and broadleaf deciduous tree types (G. B. Bonan et al., 1992). Needleleaf trees have dark leaves (low albedo) and low transpiration rates (Chapin et al., 2000). They comprise the later successional stages of the ecosystem and are characterized by slow growth rates (Van Cleve et al., 1996). By contrast, deciduous broadleaf trees in Boreal forests are relatively bright (higher albedo) with higher transpiration rates (Chapin et al., 2000). They grow back quickly following disturbance and can dominate the ecosystem following a stand-replacing disturbance event for a few hundred years (Van Cleve et al., 1996; Rupp et al., 2000), with consequences for surface energy partitioning (Liu et al., 2005). Although needleleaf trees are conceptualized as, and often are, the dominant species in the ecosystem, pollen records suggest that boreal forests in Alaska were dominated by deciduous broadleaf vegetation following the last ice age (Edwards et al., 2005). Simulations suggest this could occur again in the next century as fire frequency and intensity increases and shifts ecosystems towards early successional plant types (Rupp et al., 2000).

Vegetation plays a large role in setting the terrestrial surface climate in the Arctic by altering the surface energy budget through the exchanges of mass and energy between the land and the atmosphere. It is thought that the conversion of tundra to forests in the Arctic will contribute substantially to high-latitude warming trends due to a decrease in albedo (Chapin et al., 2005), particularly as dark trees cover bright snow. Given that vegetation is expected to move poleward during warmer climates, we expect this migration to have a positive feedback on surface temperatures through the effect of albedo.

Observations and simulations of an expansion of Arctic trees suggest that warmer temperatures at high latitudes have been driven primarily by the impact of a darker surface (G. B. Bonan et al., 1992; Thomas & Rowntree, 1992; Foley et al., 1994; Chapin et al., 2005; G. B. Bonan, 2008; Falloon et al., 2012; Collins et al., 2013; Chae et al., 2015). However, vegetation in the Arctic can also influence the surface energy budget through the flux of water to the atmosphere. The magnitude of transpiration can vary substantially across vegetation types – in particular needleleaf evergreen trees have less evapotranspiration than leafed-out deciduous broadleaf trees in the Arctic (Chapin et al., 2000).

In general, the effect of variations in plant type traits other than albedo, such as evaporative resistance (the difficulty for the plant to release water), on surface climate in the Arctic has been less well explored. Climate model simulations of an expansion of deciduous broadleaf trees (rather than needleleaf evergreen trees) at high latitudes found approximately equal amounts of warming from two distinct physical processes (Swann et al., 2010). The warming comes from both the change in albedo and the change in the greenhouse effect from elevated water vapor concentrations due to higher water flux to the atmosphere from the deciduous broadleaf trees, along with feedbacks from ocean and sea-ice (Swann et al., 2010). Other studies have focused on surface roughness and found that a change in vegetation from grasses and shrubs to needleleaf evergreen trees increases temperature due to the change in roughness which induces a cloud feedback (Cho et al., 2018), but they do not explore the changes in evaporative resistance, which we believe to be an important factor to influencing the Arctic climate (Swann et al., 2010; Laguë et al., 2019)

Swann et al. (2010) demonstrate that trees with different transpiration rates can have a significant influence on the Arctic climate, however it remains unclear what the independent relative contributions to Arctic climate are from albedo and transpiration. With the realistic possibility that tree-line will continue to move poleward as climate warms and that the forest composition may change to more deciduous broadleaf trees due to an increase of fire frequency and intensity (Rupp et al., 2000; G. B. Bonan, 2008) and as indicated by past climates, we need to understand how these changing properties from one plant species to another can affect the Arctic climate. In this paper we address the question of how albedo and resistance to surface evapotranspiration influence surface climate in the Arctic.

2 Methods

2.1 Model Description

For this study we use climate model simulations with an idealized representation of the land surface to quantify the atmospheric and surface climate response to changes in albedo and evaporative resistance of the vegetation individually. We used the Simple Land Interface Model (SLIM; (Laguë et al., 2019)), which replaces the Community Land Model (CLM) within the Community Earth System Model (CESM; (Hurrell et al., 2013)). SLIM has a number of user controlled prescribed surface properties, including surface albedo and surface evaporative resistance akin to a bulk canopy resistance (see Supplementary Information for more detail) making it useful for independently modifying surface properties in order to analyze the effects of a change in a single surface property. This is in contrast to a complex land surface model such as CLM, where a change in vegetation results in simultaneous changes to many surface properties. For example, we can specify the snow-free surface albedo directly in SLIM, while in CLM the surface albedo is an emergent property of flat leaf albedo values, leaf area, etc.. SLIM conserves energy, and evaluates the surface energy budget at each time step to determine a new surface temperature, soil temperature profile, and net fluxes of shortwave radiation, longwave radiation, sensible heat, and latent heat. Through CESM, SLIM is then coupled with the Community Atmosphere Model v. 5 (CAM5; (Neale et al., 2012)), a slab ocean model ((Neale et al., 2012)), and an interactive sea ice model (CICE; (Hunke et al., 2017)). We run our simulations globally at a resolution of 1.9° latitude by 2.5° longitude.

It is important to note that there is substantial disagreement between different land models for the robustness of biophysical climate responses to vegetation change (De Noblet-Ducoudré et al., 2012). While land surface models generally agree with each other, as well as with observations, on the effects of vegetation change on radiative fluxes, there is a much larger disagreement on how vegetation change should impact the partitioning of turbulent energy into sensible and latent heat fluxes (Duveiller et al., 2018; De Noblet-Ducoudré et al., 2012). In addition, atmospheric responses to vegetation change are substantial (Laguë et al., 2019), which means that models have a large uncertainty in the impact of vegetation change on near surface climate not only from differences in the land models and their flux representations, but also in the sensitivity of various atmospheric models to changes in land surface fluxes. Both factors (bias in turbulent fluxes and atmospheric responses) contribute to substantial differences in near-surface air temperature over land (Ma et al., 2018).

2.2 Simulations

In our simulations we set the land surface in the Arctic (north of 60°N) to have uniform prescribed values for evaporative resistance and snow-free albedo corresponding to two plant types: evergreen needleleaf and deciduous broadleaf trees. We chose representative values for the albedo and evaporative resistance for each tree type by estimating them from grid cells dominated by our two plant types in a coupled land-atmosphere simulation using CLM. Needleleaf trees have a lower albedo and a higher evaporative resistance relative to broadleaf trees (Table S1). Albedo values are specified for four streams of radiation (visible direct light, visible diffuse light, near infrared direct light, near infrared diffuse light). Our idealized land model configuration allows us to independently change a single surface property, and therefore run simulations with a factorial combination of different values for albedo and evaporative resistance. For two of our four simulations, we have the plant type traits set to replicate needleleaf and broadleaf trees - that is, one simulation has needleleaf values for both albedo and evaporative resistance, while the other has broadleaf values for both properties (Fig. S1). The two additional simulations have 'hybrid' plant types with the albedo of one tree type paired with the evaporative resistance of the other, resulting in a brighter needleleaf tree and a darker broadleaf tree. For simplicity we will refer to our four simulations as "Needleleaf" and "Broadleaf", for tree types with the observed combinations of albedo and resistance, and "Bright Needleleaf", and "Dark Broadleaf" for our hybrid tree types. The surface properties (albedo and evaporative resistance) are applied uniformly across all non-glaciated land areas north of 60°N. That is, we effectively impose a mono-culture of each tree type across the entire Arctic region in each simulation, regardless of the present-day vegetation type at each Arctic land location. Outside of the Arctic, surface properties reflect those of the present-day vegetation growing in each location and are identical in all simulations.

We use summertime values derived from a CLM simulation where we take the June-July-August surface properties in the Northern Hemisphere and the December-January-February surface properties in the Southern Hemisphere. We choose summertime in order to capture snow-free albedo values and growing season resistance values. The aerodynamic roughness of the land surface, which modulates the exchange of turbulent energy (sensible and latent heat) between the land and the atmosphere, is parametrized as a function of vegetation height and is held fixed in time (varies spatially) in all simulations. SLIM contains a simple snow model which allows for the prescribed bare-ground albedo to be masked by snow. Atmospheric CO2 concentrations are set to a constant value of 367 ppm.

We run our simulations for 50 years, using the last 30 years for analysis and omitting the first 20 years to account for spin-up (see Supporting Information, Fig. S2).

2.3 Analysis

We focus our analysis on the summer months of June, July, and August, as these months have the least amount of snow cover, thus allowing us to observe the impact of the actual snow-free surface properties on the coupled climate system. Results are presented as area-weighted averages for all Arctic land surfaces (regions north of 60°N) unless otherwise noted. We report ranges of values of one standard deviation of variability in time. Significance is calculated using a student's t-test and indicated by stippling. To account for lagged autocorrelation of up to two years, we assume N/2=15 degrees of freedom for the N=30-year period; we find this to be a conservative estimate of the actual degrees of freedom in the model using methods from Bretherton et al. (1999) (see Supporting Information, Fig. S3, S4). A p-value of 0.05 or less indicates a significant difference with 95% confidence. Given that we have four experiments but no explicit 'control' run in the classic sense, we have in some cases compared three of the experiments to a baseline of the Needleleaf tree type simulation (needleleaf albedo and needleleaf evaporative resistance), in order to see how the runs compared to one another.

To illustrate if changes in moisture or temperature are causing cloud responses we use relative humidity as a proxy for cloudiness and analyze the differences in the vertical profile of relative humidity between simulations. We partition the contribution into two parts, one from differences in temperature (T), and another from differences in specific humidity (q). We report the change in the contribution of each term relative to the normal Needleleaf run as follows:

$$\Delta RH_T = \frac{q_{ctrl}}{qsat_{exp}} - \frac{q_{ctrl}}{qsat_{ctrl}} \tag{1}$$

$$\Delta RH_q = \frac{q_{exp}}{qsat_{ctrl}} - \frac{q_{ctrl}}{qsat_{ctrl}} \tag{2}$$

where q_{ctrl} and $qsat_{ctrl}$ are the specific humidity and saturated specific humidity of the normal Needleleaf run and the q_{exp} and $qsat_{exp}$ are the specific humidity and saturated specific humidity of the other simulations that we are comparing to the normal

Needleleaf run. Equation 1 estimates the magnitude and sign of the change in the relative humidity profile between the simulations given the change in atmospheric temperature alone and Equation 2 estimates the impact given the changing specific humidity alone. The total change in relative humidity compared to the normal Needleleaf experiment also includes a small contribution from the sensitivity of actual specific humidity to temperature in the simulations. However, we are primarily focused on the dominant, independent effects of temperature and specific humidity on the relative humidity profiles in response to changing surface properties described by Equations 1 and 2 (Fig. S5).

3 Results & Discussion

Based on prior literature, we expect that higher albedo surfaces (i.e the Broadleaf and the Bright Needleleaf) will have cooler temperatures compared to lower albedo surfaces because they should absorb a smaller fraction of shortwave radiation. This assumption held true for some, but not all of our simulations. The near surface air temperatures are $\sim 2°$C cooler for the Broadleaf simulation compared to the Needleleaf (Fig. 1a). However, both the Bright Needleleaf and Dark Broadleaf simulations were $\sim 1°$C cooler than the normal Needleleaf simulation despite having different surface albedos (Fig. 1a). This suggests that additional processes are altering the surface energy budget beyond only the change in surface albedo.

3.1 Surface Energy Budget

The surface energy budget is comprised of five terms which must balance – absorbed shortwave (SW) radiation, net long wave radiation, sensible heat flux, latent heat flux, and heat storage in the ground. Averaged over the summer months, the total heat storage in the ground is comparable across all simulations and will not be part of the analysis from here on. We find that absorbed SW radiation has a similar pattern to surface temperature across experiments (Fig. 1a,b, 2a-c, g-i). Although the albedo directly affects the fraction of the incident SW radiation that the surface absorbs, the simulations with the same albedos (Needleleaf & Dark Broadleaf, Bright Needleleaf & Broadleaf) differ from one another in absorbed SW radiation by $\sim 10Wm^{-2}$ – a result that cannot be explained by changes in albedo alone (Fig. 1b). Since this difference in absorbed shortwave radiation is not due to any variation in surface albedo, it must instead be the result of changes in the amount of solar radiation reaching the surface.

The incident shortwave radiation at the surface varies substantially between the experiments with low evaporative resistance (Broadleaf and Dark Broadleaf) and the experiments with high evaporative resistance (Needleleaf and Bright Needleleaf)(Fig. 1c, S6d-f). The difference of incident shortwave radiation between high and low evaporative resistance experiments suggests that surface evaporative resistance is altering downwelling SW radiation.

The absorbed shortwave and incident SW results (Fig. 1b,c) indicate that clouds are playing a first order role in feeding back on the surface energy budget in response to changes in Arctic evaporative resistance. Incident SW radiation is very similar between simulations that have the same evaporative resistance but different surface albedo, suggesting that evaporative resistance is the dominant factor modifying incoming SW through cloud cover. Despite substantial differences in incoming SW radiation between the Dark Broadleaf and Bright Needleleaf simulations, they have a similar amount of SW radiation absorbed by the surface (Fig. 1b) and a similar change in surface temperature (Fig. 1a). This is because the darker surfaces in the Dark Broadleaf simulation absorb a larger fraction of the incident SW radiation than the Bright Needleleaf simulation (Fig. 1b,c), while the Bright Needleleaf simulation has a larger amount of incoming SW radiation due to less low cloud cover resulting from the high evaporative resistance of the land surface (Fig. 1b, 2g-i). The strong impact of changing low cloud cover on the sur-

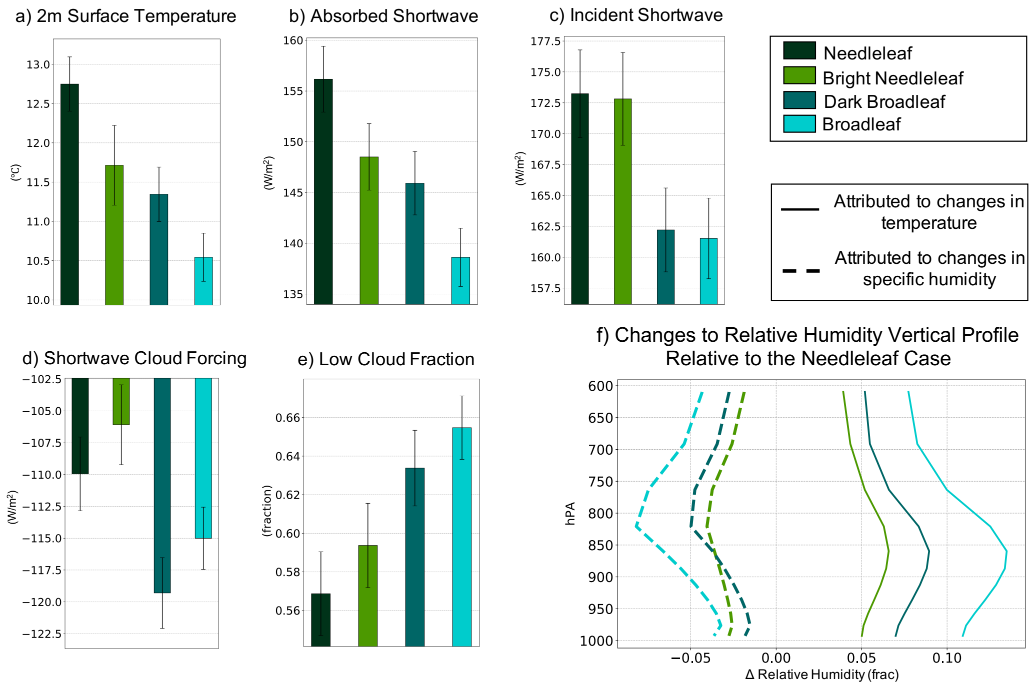

Figure 1. Arctic average fluxes, states, and cloud changes. Summertime averages over non-glaciated land North of 60°N for each of four different simulations (Needleleaf, Bright Needleleaf, Dark Broadleaf, Broadleaf) for a) 2m surface temperature (C), b) absorbed shortwave radiation at the surface (Wm^{-2}), c) incident shortwave radiation at the surface (Wm^{-2}), d) shortwave cloud forcing (Wm^{-2}) with negative values indicating more clouds, and e) low cloud fraction. The error bars represent one standard deviation of variability in time. Panel f) shows changes in the relative humidity vertical profile relative to the Needleleaf simulation attributed to changes in the vertical profile of atmospheric temperature (solid lines) and specific humidity (dashed lines).

face energy budget in our simulations is consistent with observations from the Surface Heat Budget of the Arctic (SHEBA) program and at the North Slope of Alaska Atmospheric Radiation Measurement (ARM) site, where they show that low clouds provide a net cooling in the summer through shading (Schweiger & Key, 1994; Shupe & Intrieri, 2004; Verlinde et al., 2016).

We expect simulations with lower evaporative resistances and higher amounts of total absorbed radiation (absorbed SW plus downwelling longwave) to have higher latent heat fluxes than simulations with high evaporative resistances and less total absorbed radiation. In our simulations we see that the latent heat flux is largest ($\sim 47Wm^{-2}$) for the Dark Broadleaf case, which has a high total absorbed radiation ($\sim 475Wm^{-2}$) and a low resistance to evaporation (Fig. S7a). The Bright Needleleaf simulation has a similar magnitude of total incoming radiation compared to the Dark Broadleaf simulation, but the resistance to evaporation is larger for the Bright Needleleaf simulation, leading to less latent heat flux (Fig S8b). Despite a higher evaporative resistance, the Needleleaf case has the second largest latent heat fluxes ($\sim 46Wm^{-2}$), instead of the Broadleaf case, as a result of the largest total incoming radiation $\sim 485Wm^{-2}$ (Fig. S8a,b). The relative amount of sensible heat flux across simulations, which is driven by the gradient in temperature from the surface to the atmosphere, shows a similar pattern as surface

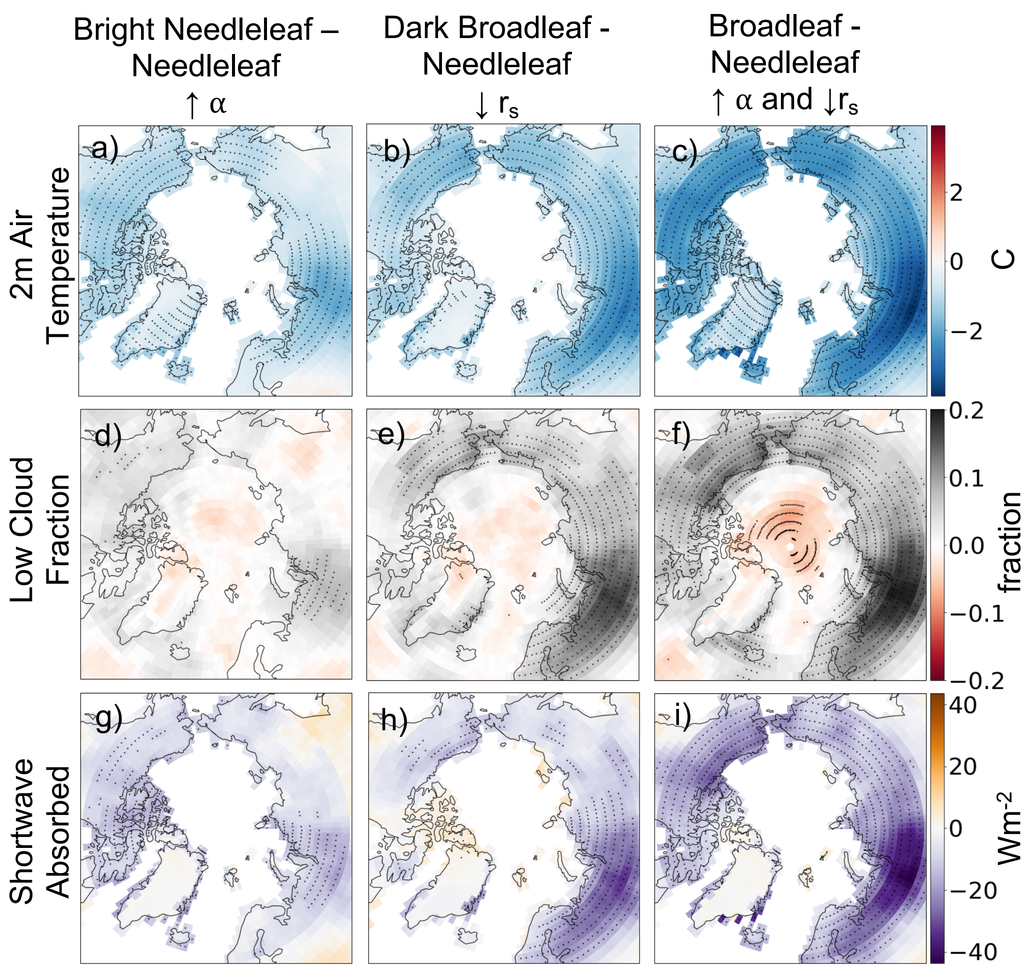

Figure 2. Spatial patterns of change over the Arctic compared to Needleleaf simulation during the Summertime. First row (a-c) shows the difference in 2m air temperature (C), the second row (d-f) shows the change in low cloud fraction, the third row (g-i) shows the change in absorbed shortwave radiation (Wm^{-2}) at the surface. Surface temperature and shortwave absorbed are plotted only over land. Column 1 shows the response to increasing albedo (α) alone (Bright Needleleaf - Needleleaf), Column 2 shows the response to decreasing evaporative resistance (r_s) alone (Dark Broadleaf - Needleleaf), and column 3 shows the response to simultaneously increasing albedo and decreasing evaporative resistance (Broadleaf - Needleleaf). Stippling indicates significance.

temperature with larger surface temperatures being associated with larger sensible heat flux, but with a greater distinction between the Bright Needleleaf and the Dark Broadleaf cases (Fig. S8c).

The Needleleaf experiment has the second largest latent heat flux despite having a high resistance to evaporation. While at first this seems surprising, it can be readily explained by the fraction of the turbulent fluxes occurring as latent heat flux (LH), defined as the Evaporative Fraction (EF):

$$EF = \frac{LH}{LH + SH} \tag{3}$$

where SH denotes Sensible Heat fluxes. We find that the low evaporative resistance simulations (Broadleaf and Dark Broadleaf) have relatively higher evaporative fractions of ~ 0.64 compared to the high evaporative resistance simulations (Needleleaf and Bright Needleleaf) which have evaporative fractions of $\sim$ 0.58 (Fig. S8d). The differences in evaporative fraction indicate that simulations with lower evaporative resistance dissipate more energy through latent heat leading to stronger cooling compared with high evaporative resistance simulations regardless of albedo.

Downwelling longwave fluxes emitted by the atmosphere toward the land surface are strongly influenced by surface temperatures (Vargas Zeppetello et al., 2019) and near-surface humidity, and have been observed to be influenced by Arctic cloud cover (Shupe & Intrieri, 2004; Verlinde et al., 2016). In our simulations with warmer surface temperatures, we also find more humid air, and more cloud cover. Thus we expect to see larger downwelling long wave radiation. We find that the greatest downwelling longwave radiation is found in the warmest simulation (Needleleaf with $\sim 330 W m^{-2}$), however the second largest downwelling longwave flux comes from the third warmest experiment (Dark Broadleaf with $\sim 328 W m^{-2}$). Based on surface temperatures alone, we would expect the Bright Needleleaf to have a larger downwelling longwave radiation than the Dark Broadleaf; however, we find that the Dark Broadleaf has more water vapor in the lower parts of the atmosphere and a larger low cloud fraction than the Bright Needleleaf (Fig. 1e, S9c, S10). Thus we hypothesize that the specific humidity and the increase of low clouds may boost the downwelling longwave radiation in the Dark Broadleaf simulation.

3.2 Clouds

The experiments with low evaporative resistance (Broadleaf and Dark Broadleaf) have a greater fraction of low clouds than experiments with high resistance (Needleleaf and Bright Needleleaf), and experiments with low albedos (Needleleaf and Dark Broadleaf) have a smaller fraction of low clouds than experiments with high albedos (Broadleaf and Bright Needleleaf) (Fig. 1e). Given the differences we observe in low cloud fraction across these experiments, we infer that changes in both albedo and evaporative resistance influence cloud formation, although the effect from the change in albedo is not as large as from the change in evaporative resistance. Cloud formation depends on the profile of relative humidity, which in turn depends both on the atmospheric temperatures and specific humidity. Both of these factors may respond to altered surface albedo and evaporative resistance. In particular, albedo and evaporative resistance may influence both the temperature of the atmosphere and the total amount of water vapor, both of which are important for cloud formation. To identify which of these factors is responsible for the change in cloud fraction that we observe in our simulations, we look at the vertical structure of relative humidity, a variable that directly describes how close the air is to saturation. We estimated the contribution to changes in the vertical structure of relative humidity from the changes in the profile of temperature and specific humidity in each of our simulations (using Equations 1&2).

Variations in relative humidity profiles between our experiments are dominated by changes in temperature (Fig. 1f). We find that most of the increase of relative humidity can be attributed to cooling of the vertical temperature profile, driven either by changes in surface albedo or evaporative resistance (Fig. 1f). Compared to the Needleleaf simulation, all other experiments show a decrease in specific humidity, which would also act to reduce the relative humidity (Fig. S10), however, this effect is secondary. We thus find that the increase in relative humidity associated with increasing low cloud cover in our lower evaporative resistance cases (Dark Broadleaf and Broadleaf) is largely driven by cooler temperature profiles in simulations with higher evaporative fraction rather than by direct changes in specific humidity. With cooler temperatures and increased low cloud fraction (Fig. 2a-f), we also find a decrease in the 500 hPa geopotential heights (Fig. S11a-c).

Cloud feedbacks occur in response to changes in both albedo and evaporative resistance, resulting in changes to shortwave cloud forcing. Shortwave cloud forcing is defined as

$$SW_{cloud\,forcing} = netSW_{all\,sky} - netSW_{clear\,sky} \tag{4}$$

where $netSW_{all\,sky}$ is the shortwave radiation at the top of the atmosphere when the radiative effect of clouds is included (all sky) and $netSW_{clear\,sky}$ is the same but using a solution from the radiative calculations in the atmospheric model as if there were no clouds present (clear sky). We find that the simulations with low evaporative resistance (Broadleaf & Dark Broadleaf) have a greater magnitude of shortwave cloud forcing than the high evaporative resistance simulations (Needleleaf & Bright Needleleaf), on average by $\sim 9Wm^{-2}$ (Fig. 1d, S6g-i). When evaporative resistance is held fixed and albedo is changed, there is still a change in shortwave cloud forcing of $\sim 4Wm^{-2}$.

Both evaporative resistance and albedo modify shortwave cloud forcing, but through different processes. Changing evaporative resistance modifies shortwave cloud forcing primarily through the total amount of low cloud cover (Fig. 1c,d), while changing albedo modifies shortwave cloud forcing through clear sky fluxes of shortwave radiation (Fig. S7b). Thus, in the case of albedo, even a relatively small change in cloud cover can result in a substantial change in shortwave cloud forcing because adding clouds above a dark surface has a greater impact on the amount of SW absorbed by the land surface than it does over a bright surface.

Earlier work by Cho et al. (2018) identified that low cloud feedbacks were an important factor in determining the surface temperature response to a change in vegetation cover in the Arctic. However it is unclear from their study how clouds would respond to a change in evaporative resistance alone. Consistent with Cho et al. (2018), we also see decreases in low cloud cover and increases in the magnitude of shortwave cloud forcing in response to a darker surface. They propose two possible explanations for the reduction in low clouds: first, a reduction in relative humidity caused by an increase in temperature, and second, an increase of roughness causing an increase in the planetary boundary layer height. In our simulations we see large differences in cloud cover and shortwave cloud forcing due to changes in evaporative resistance which we also attribute to changes in the vertical profile of temperature; however, in contrast we find a reduction in low cloud cover and an increase of surface temperature change to be driven by the evaporative fraction rather than the surface roughness. We additionally note that our experimental design using SLIM allows us to directly separate the effects of surface properties such as albedo and evaporative resistance on Arctic climate. Future simulations could potentially be used to isolate the impact of surface aerodynamic roughness, but this is not explored in this study.

3.3 Further Considerations

In this paper we have identified that changes in evaporative resistance associated with a shift in vegetation cover over the Arctic influences the evaporative fraction, resulting in cloud feedbacks which have the same order of magnitude effect on energy fluxes and surface temperature as changes in surface albedo. This explanation holds in the summer, but we find that it does not appear in winter due to the accumulated snow cover and the lack of incoming sunlight, which changes the turbulent fluxes for our simulations. However, the surface temperature pattern that we see in the summertime in our four experiments appears to persist throughout the year with a smaller magnitude. We hypothesize that the differences in the temperature over land in the wintertime are a result of differences in the simulated amount of seasonal sea ice (Fig. S12a). The differences in sea ice in each of the seasons are broadly correlated with the amount of sea ice loss in the summer (Fig. S12b), which we hypothesize to be driven by differences in summertime temperatures. Thus the differences year-round could be indirectly driven by summertime conditions.

We note that actual vegetation has seasonal variations in albedo and evaporative resistance. In this idealized study we have chosen to represent only the summer values of surface properties and are unable to parse the effect of seasonal variations in leaf area by masking snow during shoulder seasons (Cook et al., 2008; Swann et al., 2010; Bonfils et al., 2012; Luyssaert et al., 2018).

Uncertainty in the CLM parameter values used to inform our imposed change in albedo could modify our results. For example, Majasalmi and Bright (2019) find that while CLM has a reasonable representation of visible albedo for boreal plant types, the albedo in the near-infrared is underestimated. A brighter albedo for needleleaf boreal trees in the near-infrared, similar to the near-infrared albedo of broadleaf boreal trees, would reduce the total temperature effect of the change in albedo associated with a change in boreal forest type, although the effect is smaller than it would be for a bias in visible albedos.

4 Conclusions and Implications

We analyzed the effects of specified albedos and evaporative resistances associated with two common tree types in the Arctic: needleleaf evergreen trees and broadleaf deciduous trees. We find that evaporative resistance plays a large role in influencing surface air temperature over land in the Arctic, similar in magnitude to the influence of surface albedo. In simulations with lower evaporative resistance we see that there is an increase in the low cloud fraction, which in turn reduces the shortwave radiation incident at the land surface and enhances shortwave cloud forcing. The difference in incident radiation due to changes in evaporative resistance is then compounded by changes in albedo in cases where both evaporative resistance and albedo are modified, resulting in drastically different temperatures between experiments with differences in both albedo and evaporative resistance (Broadleaf and Needleleaf), and similar temperatures when either one of the surface properties is swapped (Bright Needleleaf and Dark Broadleaf). Our results show that evaporative resistance is as important in influencing Arctic surface temperatures as surface albedo and needs to be considered in future studies when trying to understand the effects of vegetation change in the Arctic. These results also demonstrate the usefulness of idealized approaches to land surface modeling (in our case with SLIM) and how we can use this modeling approach to isolate individual surface properties to quantify how changes in specific aspects of the land surface influence the larger climate system. Further studies focused on the role of specific land surface properties and their influence on Arctic climate and circulation could advance our understanding of the potential future climate impacts of high-latitude vegetation change.

Acknowledgments
We acknowledge support from the National Science Foundation AGS-1553715 to the University of Washington. We would like to acknowledge high-performance computing support from Cheyenne (doi:10.5065/D6RX99HX) provided by NCAR's Computational and Information Systems Laboratory, sponsored by the National Science Foundation. Model results are available through the University of Washington Libraries ResearchWorks digital repository at http://hdl.handle.net/1773/45281.

References

Bonan, G. (2015). *Ecological climatology: Concepts and applications* (3rd ed.). Cambridge University Press. doi: 10.1017/CBO9781107339200

Bonan, G. B. (2008). Forests and climate change: Forcings, feedbacks, and the climate benefits of forests. , *320*(5882), 1444-1449. doi: 10.1126/science.1155121

Bonan, G. B., Pollard, D., & Thompson, S. L. (1992). Effects of boreal forest vegetation on global climate. *Nature*, *359*(6397), 716-718.

Bonfils, C. J., Phillips, T. J., Lawrence, D. M., Cameron-Smith, P., Riley, W. J., & Subin, Z. M. (2012). On the influence of shrub height and expansion on northern high latitude climate. *Environmental Research Letters*. doi: 10.1088/1748-9326/7/1/015503

Bretherton, C. S., Widmann, M., Dymnikov, V. P., Wallace, J. M., & Bladé, I. (1999). The effective number of spatial degrees of freedom of a time-varying field. *Journal of Climate*. doi: 10.1175/1520-0442(1999)012⟨1990:TENOSD⟩2.0.CO;2

Chae, Y., Kang, S. M., Jeong, S. J., Kim, B., & Frierson, D. M. (2015). Arctic greening can cause earlier seasonality of Arctic amplification. *Geophysical Research Letters*. doi: 10.1002/2014GL061841

Chapin, F. S., Mcguire, A. D., Randerson, J., Pielke, R., Baldocchi, D., Hobbie, S. E., ... Running, S. W. (2000). Arctic and boreal ecosystems of western North America as components of the climate system. *Global Change Biology*. doi: 10.1046/j.1365-2486.2000.06022.x

Chapin, F. S., Sturm, M., Serreze, M. C., McFadden, J. P., Key, J. R., Lloyd, A. H., ... Welker, J. M. (2005). Role of land-surface changes in arctic summer warming. *Science*. doi: 10.1126/science.1117368

Cho, M. H., Yang, A. R., Baek, E. H., Kang, S. M., Jeong, S. J., Kim, J. Y., & Kim, B. M. (2018). Vegetation-cloud feedbacks to future vegetation changes in the Arctic regions. *Climate Dynamics*. doi: 10.1007/s00382-017-3840-5

Collins, M., Knutti, R., Arblaster, J., Dufresne, J.-L., Fichefet, T., Friedlingstein, P., ... Wehner, M. (2013). Long-term climate change: Projections, commitments and irreversibility [Book Section]. In T. Stocker et al. (Eds.), *Climate change 2013: The physical science basis. contribution of working group i to the fifth assessment report of the intergovernmental panel on climate change* (pp. 1029–1136). Cambridge, United Kingdom and New York, NY, USA: Cambridge University Press. Retrieved from `www.climatechange2013.org` doi: 10.1017/CBO9781107415324.024

Cook, B. I., Bonan, G. B., Levis, S., & Epstein, H. E. (2008). Rapid vegetation responses and feedbacks amplify climate model response to snow cover changes. *Climate Dynamics*. doi: 10.1007/s00382-007-0296-z

De Noblet-Ducoudré, N., Boisier, J. P., Pitman, A., Bonan, G. B., Brovkin, V., Cruz, F., ... Voldoire, A. (2012). Determining robust impacts of land-use-induced land cover changes on surface climate over North America and Eurasia: Results from the first set of LUCID experiments. *Journal of Climate*. doi: 10.1175/JCLI-D-11-00338.1

Duveiller, G., Forzieri, G., Robertson, E., Li, W., Georgievski, G., Lawrence, P., ... Cescatti, A. (2018). Biophysics and vegetation cover change: A process-based evaluation framework for confronting land surface models with satellite observations. *Earth System Science Data*. doi: 10.5194/essd-10-1265-2018

Edwards, M., Brubaker, L., Lozhkin, A., & Anderson, P. (2005). Structurally novel biomes: A response to past warming in beringia. *Ecology*, *86*(7), 1696-1703.

Falloon, P. D., Dankers, R., Betts, R. A., Jones, C. D., Booth, B. B. B., & Lambert, F. H. (2012). Role of vegetation change in future climate under the a1b scenario and a climate stabilisation scenario, using the hadcm3c earth system model. *Biogeosciences*, *9*(11), 4739–4756. doi: 10.5194/bg-9-4739-2012

Foley, J. A., Kutzbach, J., Coe, M. T., & Levis, S. (1994). Feedbacks between climate and boreal forests during the holocene epoch. *Nature*, *371*(6492), 52-54.

Gallimore, R., Jacob, R., & Kutzbach, J. (2005). Coupled atmosphere-ocean-vegetation simulations for modern and mid-Holocene climates: Role of extratropical vegetation cover feedbacks. *Climate Dynamics*. doi: 10.1007/s00382-005-0054-z

Hunke, E., Lipscomb, W., Jones, P., Turner, A., Jeffery, N., & Elliott, S. (2017). *Cice, the los alamos sea ice model, version 00.* Retrieved from `https://www.osti.gov//servlets/purl/1364126`

Hurrell, J. W., Holland, M. M., Gent, P. R., Ghan, S., Kay, J. E., Kushner, P. J., ... Marshall, S. (2013). The community earth system model: A framework for collaborative research. *Bulletin of the American Meteorological Society*, *94*(9), 1339–1360. Retrieved from `http://dx.doi.org/10.1175/BAMS-D-12-00121.1` doi: 10.1175/BAMS-D-12-00121.1

Jeong, S. J., Ho, C. H., Park, T. W., Kim, J., & Levis, S. (2011). Impact of vegetation feedback on the temperature and its diurnal range over the Northern Hemisphere during summer in a 2 CO2 climate. *Climate Dynamics*. doi: 10.1007/s00382-010-0827-x

Laguë, M. M. L., Bonan, G. B., & Swann, A. L. S. (2019). Separating the impact of individual land surface properties on the terrestrial surface energy budget in both the coupled and un-coupled land-atmosphere system. *Journal of Climate*.

Liu, H., Randerson, J., Lindfors, J., & Chapin, F. (2005). Changes in the surface energy budget after fire in boreal ecosystems of interior alaska: An annual perspective. *Journal of Geophysical Research-Atmospheres*, *110*. doi: ARTND13101

Lloyd, A. H. (2005). Ecological histories from Alaskan tree lines provide insight into future change. *Ecology*. doi: 10.1890/03-0786

Luyssaert, S., Marie, G., Valade, A., Chen, Y. Y., Njakou Djomo, S., Ryder, J., ... McGrath, M. J. (2018). *Trade-offs in using European forests to meet climate objectives.* doi: 10.1038/s41586-018-0577-1

Ma, H. Y., Klein, S. A., Xie, S., Zhang, C., Tang, S., Tang, Q., ... Wang, Y. C. (2018). CAUSES: On the Role of Surface Energy Budget Errors to the Warm Surface Air Temperature Error Over the Central United States. *Journal of Geophysical Research: Atmospheres*. doi: 10.1002/2017JD027194

Majasalmi, T., & Bright, R. M. (2019). Evaluation of leaf-level optical properties employed in land surface models. *Geoscientific Model Development*, *12*(9), 3923-3938. doi: 10.5194/gmd-2019-59

Neale, R. B., Gettelman, A., Park, S., Chen, C.-c., Lauritzen, P. H., Williamson, D. L., ... Taylor, M. a. (2012). Description of the NCAR Community Atmosphere Model (CAM 5.0). *Ncar/Tn-464+Str*. doi: 10.5065/D6N877R0.

Royer, D. L., Osborne, C. P., & Beerling, D. J. (2006). Contrasting seasonal patterns of carbon gain in evergreen and deciduous trees of ancient polar forests. *Paleobiology*. doi: 10.1666/0094-8373(2005)031⟨0141:cspocg⟩2.0.co;2

Rundqvist, S., Hedenås, H., Sandström, A., Emanuelsson, U., Eriksson, H., Jonasson, C., & Callaghan, T. V. (2011). *Tree and shrub expansion over the past 34 years at the tree-line near Abisko, Sweden.* doi: 10.1007/s13280-011-0174-0

Rupp, T. S., Chapin, F. S., & Starfield, A. M. (2000). Response of subarctic vegetation to transient climatic change on the Seward Peninsula in north-west Alaska. *Global Change Biology*. doi: 10.1046/j.1365-2486.2000.00337.x

Schweiger, A. J., & Key, J. R. (1994). Arctic ocean radiative fluxes and cloud forcing estimated from the isccp c2 cloud dataset, 1983-1990. *Journal of Applied Meteorology*, *33*(8), 948-963.

Shupe, M. D., & Intrieri, J. M. (2004). Cloud radiative forcing of the Arctic surface: The influence of cloud properties, surface albedo, and solar zenith angle. *Journal of Climate*. doi: 10.1175/1520-0442(2004)017⟨0616:CRFOTA⟩2.0.CO;2

Swann, A. L., Fung, I. Y., Levis, S., Bonan, G. B., & Doney, S. C. (2010). Changes in arctic vegetation amplify high-latitude warming through the greenhouse effect. *Proceedings of the National Academy of Sciences of the United States of*

America, *107*(4), 1295-1300. doi: DOI10.1073/pnas.0913846107

Thomas, G., & Rowntree, P. R. (1992). The Boreal Forests and Climate. *Quarterly Journal of the Royal Meteorological Society*. doi: 10.1002/qj.49711850505

Van Cleve, K., Viereck, L. A., Dyrness, C. T., & VanCleve, K. (1996). State factor control of soils and forest succession along the Tanana River in interior Alaska, USA. *Arctic and Alpine Research*.

Vargas Zeppetello, L. R., Donohoe, A., & Battisti, D. S. (2019). Does Surface Temperature Respond to or Determine Downwelling Longwave Radiation? *Geophysical Research Letters*. doi: 10.1029/2019GL082220

Verlinde, J., Zak, B. D., Shupe, M. D., Ivey, M. D., & Stamnes, K. (2016). The ARM North Slope of Alaska (NSA) Sites. *Meteorological Monographs*. doi: 10.1175/amsmonographs-d-15-0023.1

Wolfe, J. A., & Upchurch, G. R. (1987). North American nonmarine climates and vegetation during the Late Cretaceous. *Palaeogeography, Palaeoclimatology, Palaeoecology*. doi: 10.1016/0031-0182(87)90040-X